SUPPORTING INFORMATION FOR

Chemical-chemical redox cycling amplification strategy in self-powered photoelectrochemical system: A proof of concept for signal amplified photocathodic immunoassay

Jing-Lu Lv,[a] Bing Wang,[a] Xiao-Jing Liao,[a] Shu-Wei Ren,[b] Jun-Tao Cao,*[a] and Yan-Ming Liu*[a]

[a]College of Chemistry and Chemical Engineering, Institute for Conservation and Utilization of Agro-bioresources in Dabie Mountains, Xinyang Normal University, Xinyang 464000, China

[b]Xinyang Central Hospital, Xinyang 464000, China

* To whom correspondence should be addressed.

* E-mail: liuym9518@sina.com; jtcao11@163.com

Tel & fax: +86-376-6392889

Contents

Part 1: Experimental

Materials. IL-6 and anti-IL-6 polyclonal antibody were purchased from Shanghai Linc-Bio Science Co., Ltd. (Shanghai, China). Human serum albumin (HSA), bovine serum albumin (BSA), and human IgG were bought from Shanghai Solarbio Bioscience & Technology Co., Ltd (Shanghai, China). ALP and 4-aminophenyl phosphate (APP) monosodium salt hydrate were ordered from Apollo Scientific Ltd. (Manchester, UK). 4-aminophenol (AP), β-nicotinamide adenine dinucleotide reduced dipotassium (NADH), and ascorbic acid (AA) were obtained from Sigma-Aldrich (St. Louis, MO). $TaCl_5$, $Bi(NO_3)_3 \cdot 5H_2O$, $CuCl_2$, $InCl_3$, and glutaraldehyde (GLD) were provided by Shanghai Macklin Biochemical Co., Ltd (China). $AgNO_3$, chitosan (CS) powder (from crab cells, 85% deacetylation), $Na_2S \cdot 9H_2O$, Tween-20, aminopropyltriethoxysilane (APTES), and SiO_2 nanoparticles (99.5%, 30 nm) were from Aladdin Reagent Inc. (Shanghai, China). All chemicals were of analytical grade. The aqueous solutions were prepared with ultrapure water (18.2 MΩ·cm) from Aike water treatment solution provider (China).

Phosphate buffer solution (PBS, 0.01 M, pH 7.4) was used for the preparation of the antibody and antigen solution. The attenuation and usage of ALP were performed in Tris-HCl (0.01 M, pH 8.0) including 5.0 mM $MgCl_2$ and 0.2 mM $ZnCl_2$. The Tris-HNO_3 buffer (pH 9.0) for enzymatic reaction contained 50 mM Tris and 10 mM $Mg(NO_3)_2$, and the pH value was regulated by HNO_3.

Apparatus. The cyclic voltammogram (CV), and electrochemical impedance spectroscopy (EIS) were obtained on a RST5200 electrochemical workstation (Zhengzhou Shiruisi Technology Co., Ltd., China) with a three-electrode system in 5.0 mM $K_3[Fe(CN)_6]/K_4[Fe(CN)_6]$ (1:1) mixture containing 0.1 M KCl. The morphologies of the samples were observed with a field emission scanning electron microscope (SEM, Hitachi, S-4800, Japan). X-ray photoelectron spectra (XPS) images were recorded on a K-Alpha X-ray photoelectron spectrometer (Thermo Fisher Scientific Co., USA). Transmission electron microscopy (TEM) images were

taken on a FEI Tecnai G2 F20 electron microscope operated at 200 kV. The UV-vis absorption spectra were recorded on a PerkinElmer Lambda 950 UV−Vis spectrophotometer (Shimadzu, Japan). Powder X-ray diffraction (XRD) was recorded on a Rigaku Smartlab 9KW X-ray diffractometer (Japan, Cu Kα radiation, λ = 1.5406 Å).

The self-powered detection device was constructed by using a two-compartment cell with a Nafion 117 membrane as separator. The Bi_2S_3/Bi_3TaO_7 heterojunction-based photoelectrode and $CuInS_2$-based photoelectrode were separately dipped into the two compartments of the detection device served as photoanode and photocathode, respectively. The CHI660E electrochemical workstation (Shanghai Chenhua Apparatus Corporation, China) was used to record the photocurrent responses produced by the two-electrode system and a white light with a spectral range from 400 to 700 nm from a 3 W LED lamp was utilized as stimulus light to irradiate both the photoanode and the photocathode. The distance between the light source and the electrode surface was 10 cm and the stimulus light was switched on and off every 10 s. The external voltage was 0.0 V.

Preparation of the Bi_2S_3/Bi_3TaO_7 heterojunction-based photoanode. Bi_3TaO_7 nanoparticles (NPs) and Bi_2S_3 nanorods (NRs) were first prepared according to the literatures.[1,2] The Bi_2S_3/Bi_3TaO_7 heterojunction was prepared by directly mixing Bi_3TaO_7 NPs with Bi_2S_3 NRs according to a certain proportion in water and then ultrasonication for 30 min. To fabricate the photoanode, the bare electrodes were ultrasonicated for 10 min in acetone solution, ultrapure water, ethanol solution and ultrapure water, respectively, and then dried at 120 °C for 2 h. 20 μL of the above mentioned Bi_2S_3/Bi_3TaO_7 suspension (Bi_3TaO_7 : Bi_2S_3 = 1:3, 3 mg/mL) was then dropped onto the surface of the cleaned ITO electrode with an exposed geometric area of 0.25 cm^2, and then dried in an oven at 60 °C. Finally, the Bi_2S_3/Bi_3TaO_7/ITO electrode was acquired and used as photoanode.

Preparation of the $CuInS_2$ microflowers-based photocathode. $CuInS_2$ was synthesized by a hydrothermal method.[3] Typically, 40 mL of ethylene glycol solution containing 0.03 M $CuCl_2$ (copper source), 0.03 M $InCl_3$ (indium source), and 0.12 M

thiourea (sulfur source), was transferred to a 50 mL polytetrafluoroethylene lined autoclave. After reaction for 24 h at 200 °C, the black precipitates of $CuInS_2$ micro-flowers were acquired. The precipitates were washed several times with ultrapure water and ethanol, and then dried at 60 °C overnight. To fabricate the photocathode, 6 mg/mL of the $CuInS_2$ solution (20 μL) containing 1wt% CS and 1% acetic acid was spread on the surface of the cleaned ITO electrode with an exposed geometric area of 0.25 cm^2 and the photocathode was fabricated after drying the modified electrode at 60 °C.

Preparation of the Anti-IL-6-SiO_2-ALP. The anti-IL-6-SiO_2-ALP probe was synthesized as follows. Firstly, the SiO_2 was aminated with APTES, and then functionalized with aldehyde group with GLD. Secondly, 400 μL anti-IL-6 (15 μg/mL) and 400 μL ALP (30 μg/mL) were pre-mixed and added to 400 μL aldehyde group functionalized SiO_2 solution. After 1 h reaction at 37 °C under gently stirring, the mixture was centrifuged and dispersed in 400 μL PBS. Thirdly, 0.01 M PBS solution (pH 7.4) containing 1% (w/v) BSA was used to block nonspecific binding sites for 1 h at 37 °C. Subsequent to centrifugation and washing, the anti-IL-6-SiO_2-ALP probe was redispersed in 400 μL PBS and stored at 4 °C before use.

PEC measurements. The PEC analysis was carried out in a split-type mode. The AP obtained from the enzyme catalytic reaction in the 96-well plate was immediately transferred into the Tris-HNO_3 buffer containing 1.0 mM $AgNO_3$ and 1.0 mM NADH on the $CuInS_2$/ITO-based photocathode. The redox cycling process on the photocathode was achieved for 10 min incubation. After rinsing the photocathode with Tris-HNO_3 buffer and water thoroughly, the electrode was assembled with the photoanode to construct the self-powered device for PEC measurements. The PBS (pH 7.4, 0.01 M) and that containing 0.1 M AA was used as the detection solution in the photocathodic and photoanodic cells, respectively. In the PEC measurements, the stimulus light was switched on and off every 10 s.

Part 2: Scheme 1B

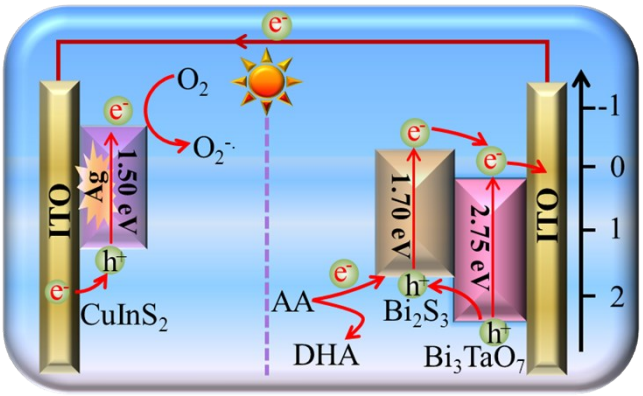

Scheme 1B. Photogenerated electron-hole transfer process of the PEC system.

Part 3: XPS of the photoanode

The surface composition and oxidation state of various elements in the prepared Bi_2S_3/Bi_3TaO_7 heterojunction were further studied by XPS measurement. It can be observed from the entire XPS spectrum that the product is mainly composed of Bi, Ta, O, S, C elements (Figure S1A). In Figure S1B, the predominant peaks at 158.18 eV and 163.50 eV are identified at Bi $4f_{7/2}$ and Bi $4f_{5/2}$, respectively, confirming the existence of Bi^{3+}, meanwhile the binding energy at 160.81 eV is responsible for the S $2p_{3/2}$ of S^{2-}. In Figure S1C, the peaks at 28.08 eV and 25.18 eV are ascribed to Ta $4f_{5/2}$ and Ta $4f_{7/2}$ of Ta^{5+}, respectively. Consequently, the successful synthesis of Bi_2S_3/Bi_3TaO_7 heterojunction is further verified.

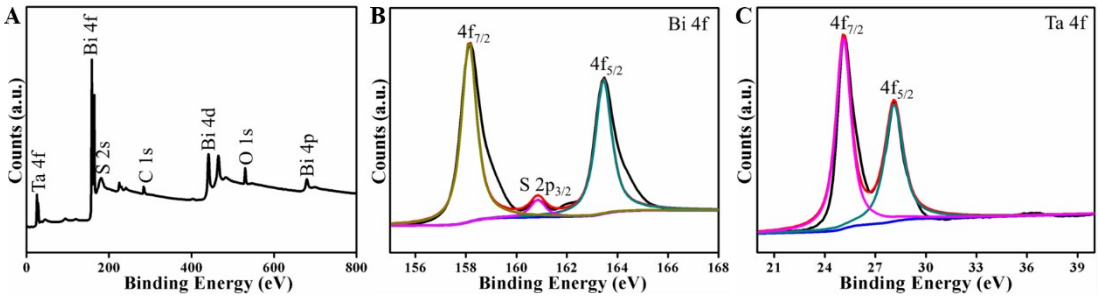

Fig. S1. (A) Survey XPS spectrum, high-resolution XPS spectra of Bi_2S_3/Bi_3TaO_7 (B) Bi 4f and S 2p; (C) Ta 4f.

Part 4: SEM, XRD, and UV-vis absorption spectrum of the photocathode

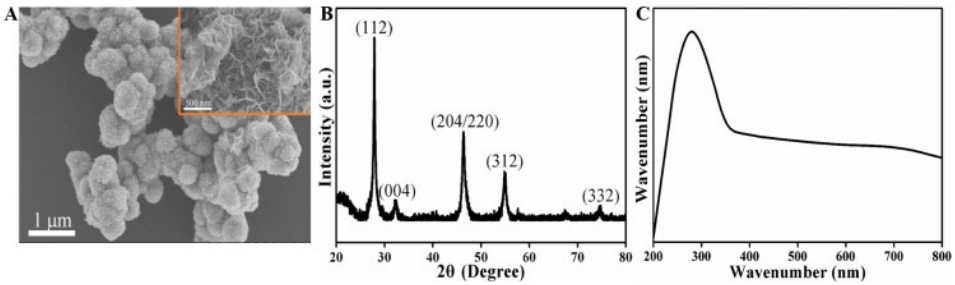

Figure S2. (A) SEM images of $CuInS_2$ at low and high (inset in A) magnification; (B) XRD pattern; and (C) UV-vis absorption spectra of $CuInS_2$.

Part 5: Optimization of experimental conditions

As the photoactive material for the photoanode construction, the $Bi_2S_3/Bi_2Sn_2O_7$ heterojunction in terms of the mass ratio and the concentration was firstly optimized. Figure S3A displays the photocurrent responses of 2.0 mg/mL Bi_2S_3/Bi_2TaO_7 heterojunction at different mass ratio of Bi_3TaO_7 to Bi_2S_3. It can be seen that the photocurrent response of Bi_2S_3/Bi_2TaO_7 reached the highest value at the mass ratio of 1:3 ($m_{Bi3TaO7}$:m_{Bi2S3}). Then, the PEC behaviors of Bi_2S_3/Bi_2TaO_7 at different concentrations ($m_{Bi3TaO7}$:m_{Bi2S3} = 1:3) were investigated. As shown in Figure S3B, the maximum PEC response was observed at the concentration of 3 mg/mL. Therefore, 3

mg/mL of Bi_2S_3/Bi_2TaO_7 heterojunction at the mass ratio of 1:3 ($m_{Bi3TaO7}$:m_{Bi2S3}) was selected for the subsequent photoanode preparation.

The concentration of $CuInS_2$ for photocathode construction was also studied. It can be seen from Figure S3C that the concentration of $CuInS_2$ at 6.0 mg/mL could achieve the highest photocurrent responses compared to the other concentrations of $CuInS_2$. So, 6.0 mg/mL $CuInS_2$ was used for the subsequent photocathode construction.

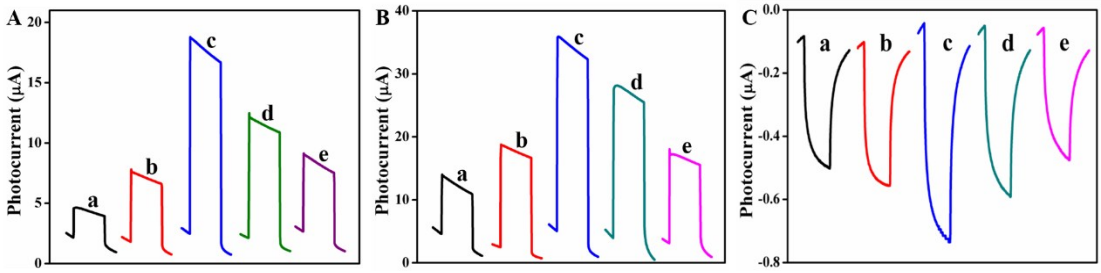

Fig. S3. PEC responses of Bi_2S_3/Bi_2TaO_7/ITO in PBS solution including 0.1 M AA with (A) various mass ratios of Bi_3TaO_7 to Bi_2S_3 at 2.0 mg/mL: 1:1 (curve a); 1:2 (curve b); 1:3 (curve c); 1:4 (curve d); 1:5 (curve e), and (B) varied concentrations: 1.0 mg/mL (curve a); 2.0 mg/mL (curve b); 3.0 mg/mL (curve c); 4.0 mg/mL (curve d); 5.0 mg/mL (curve e). (C) Photocurrent responses of the $CuInS_2$/ITO cathode prepared with different concentrations of $CuInS_2$ suspension, varied concentrations: 4.0 mg/mL (curve a); 5.0 mg/mL (curve b); 6.0 mg/mL (curve c); 7.0 mg/mL (curve d); 8.0 mg/mL (curve e). In PEC measurements, the stimulus light was switched on and off every 10 s.

Part 6: SEM and EDX images of Ag/$CuInS_2$ on photocathode

The presence of Ag on the $CuInS_2$ was characterized by SEM and EDX measurement, respectively. The Figure S4B exhibits the Ag particles were decorated on the $CuInS_2$ surface, indicating that Ag nanoparticles were successfully deposition on the $CuInS_2$. The EDX image of the $CuInS_2$ (Figure S4C), indicating that the sample was mainly composed of Cu, In, and S elements. Figure S4D display that the chemical composition of the Ag/$CuInS_2$, the result demonstrates that Ag element existed on the $CuInS_2$.

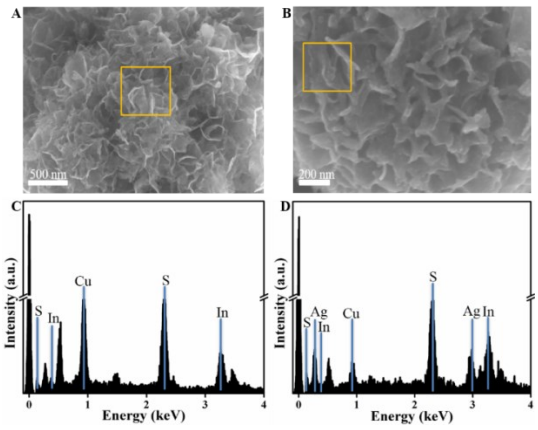

Fig. S4. SEM images and the corresponding energy-dispersive X-ray (EDX) spectra of $CuInS_2$/ITO photocathode before (A, C) and after Ag (B, D) deposition, respectively.

Part 7: XPS spectra of the $CuInS_2$ and Ag/$CuInS_2$

The chemical state of Ag on the $CuInS_2$ was also studied by XPS analysis. The survey spectra in Figure S5A indicate the presence of Cu, In, and S elements in the $CuInS_2$ and Ag/$CuInS_2$. Moreover, the diffraction peak of Ag could be clearly observed in the Ag/$CuInS_2$, which consistent with EDX images. The XPS spectra of Ag 3d state contained two peaks at 368.16 eV and 374.16 eV should be assigned to $3d_{5/2}$ and $3d_{3/2}$, respectively (Figure S5B), demonstrating the existence of Ag (0).[4] These results could prove the Ag was successfully deposited on $CuInS_2$ surface. As shown in Figure S5C and Figure S5C', the peaks at 444.47 eV and 452.04 eV correspond to the In $3d_{5/2}$ and In $3d_{3/2}$, respectively. The XPS survey of $CuInS_2$ is seen to be very similar to those for Ag/$CuInS_2$, indicating that the decoration of Ag nanoparticles onto $CuInS_2$ cannot lead to an evident change in the elemental oxidation state. It can be deduced that there is no possible reaction between the Ag^+/Ag and $CuInS_2$.

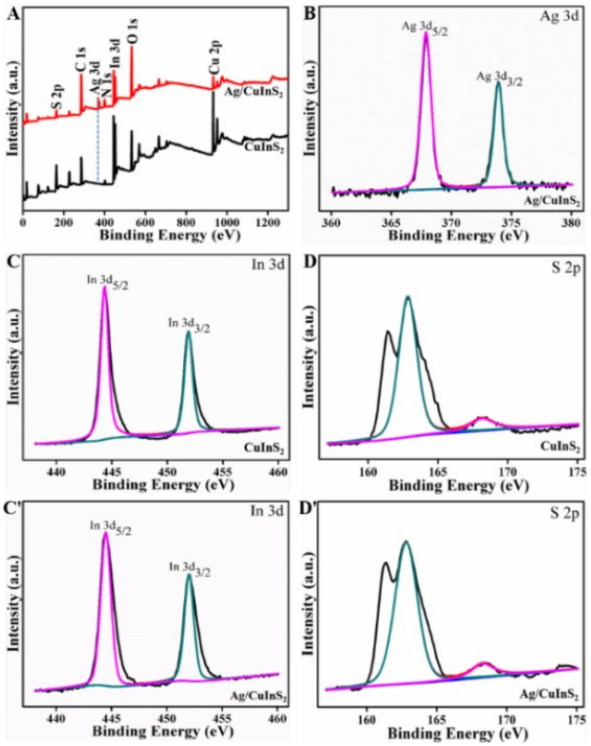

Fig. S5. XPS spectra of the $CuInS_2$ and $Ag/CuInS_2$: (A) the full survey spectrum; (B) Ag 3d; (C and C') In 3d; and (D and D') S 2p.

Part 8: EIS and PEC characterization of the chemical-chemical redox cycling amplification

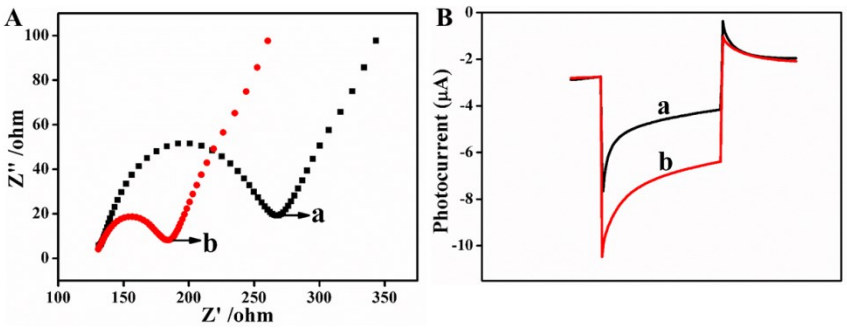

Fig. S6. (A) EIS and (B) photocurrent responses of the $CuInS_2$/ITO electrode before and after redox cycling process.

Part 9: Selectivity

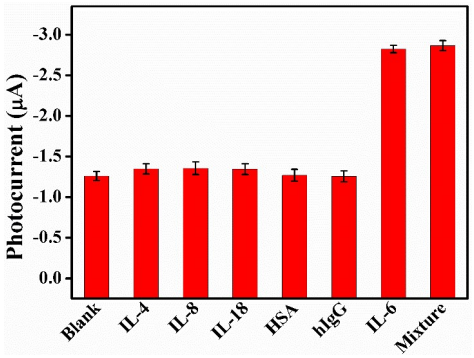

Fig. S7. Selectivity of the PEC system. The concentrations of IL-4, IL-8, IL-18, HSA, hIgG, IL-6 are 1.0×10^{-10}, 1.0×10^{-10}, 1.0×10^{-10}, 4.0×10^{-2}, 1.0×10^{-2}, and 1.0×10^{-10} g/mL, respectively.

Part 10: Table S1 The comparison of the proposed method with the previously reported methods for IL-6 detection.

Analytical methods	Linear ranges (pg mL^{-1})	Detection limits (pg mL^{-1})	References
Anodic PEC method	500 - 10000	500	5
Anodic PEC method	10 - 60000	3.4	6
Cathodic PEC method	0.1 - 500000	0.037	7
Integrating photoanode with photocathode	5 - 500000	1.8	8
Integrating photoanode with photocathode	0.05 - 10000	0.02	This work

Part 11: Table S2 Analytical results of the proposed method for IL-6 in human serum samples.

Serum Samples No.	This work (pg mL^{-1})	RSDs (%, n = 3)
1	0.170	5.5
2	0.186	4.8
3	0.603	6.1
4	1.230	7.6
5	1.905	6.0

Part 12: Table S3 Recovery of IL-6 in human serum samples.

Serum samples No.	Found (pg mL^{-1})	Added (pg mL^{-1})	Total found (pg mL^{-1})	Recovery (%)	RSDs (%, n = 3)
1	0.170	0.01	0.180	110.0	6.6
		0.10	0.263	93.0	5.3
		1.00	1.174	100.4	4.1
2	1.905	0.10	2.001	96.0	7.9
		1.00	2.765	86.0	5.9
		10.0	12.218	103.13	4.7

Part 13: Reference

(1) J. T. Cao, B. Wang, Y. X. Dong, Q. Wang, S. W. Ren, Y. M. Liu and W. W. Zhao, *ACS Sens*., 2018, **3**, 1087-1092.

(2) B. Luo, M. Chen, Z. Zhang, J. Xu, D. Li, D. B. Xu and W. D. Shi, *Dalton Trans*., 2017, **46**, 8431-8438.

(3) G. C. Fan, Y. W. Lu, H. Zhao, Q. Y. Liu, Z. M. Li and X. L. Luo, *Biosens. Bioelectron*., 2019, **137**, 52-57.

(4) Z. Z. Cheng, X. Y. Zhan, F. M. Wang, Q. S. Wang, K. Xu, Q. L. Liu, C. Jiang, Z.

X. Wang and J. He, *RSC Advances*., 2015, **5**, 81723-81727.

(5) W. W. Zhao, Z. Y. Ma, D. Y. Yan, J. J. Xu and H. Y. Chen, *Anal. Chem*., 2012, **84**, 10518-10521.

(6) G. C. Fan, L. Han, J. R. Zhang and J. J. Zhu, *Anal. Chem*., 2014, **86**, 12398-12405.

(7) L. X. Liu, G. C. Fan, J. R. Zhang and J. J. Zhu, *Analytica Chimica Acta.* 2018, **1027**, 33-40.

(8) G. C. Fan, L. Z. Ma, S. Jayachandran, Z. M. Li and X. L. Luo, *Chem. Commun*., 2018, **54**, 7062-7065.